JB Journals.ASM.org

FlgM Is Secreted by the Flagellar Export Apparatus in *Bacillus subtilis*

Rebecca A. Calvo, Daniel B. Kearns

Indiana University, Department of Biology, Bloomington, Indiana, USA

The bacterial flagellum is assembled from over 20 structural components, and flagellar gene regulation is morphogenetically coupled to the assembly state by control of the anti-sigma factor FlgM. In the Gram-negative bacterium *Salmonella enterica*, FlgM inhibits late-class flagellar gene expression until the hook-basal body structural intermediate is completed and FlgM is inhibited by secretion from the cytoplasm. Here we demonstrate that FlgM is also secreted in the Gram-positive bacterium *Bacillus subtilis* and is degraded extracellularly by the proteases Epr and WprA. We further demonstrate that, like in *S. enterica*, the structural genes required for the flagellar hook-basal body are required for robust activation of σ^D-dependent gene expression and efficient secretion of FlgM. Finally, we determine that FlgM secretion is strongly enhanced by, but does not strictly require, hook-basal body completion and instead demands a minimal subset of flagellar proteins that includes the FliF/FliG basal body proteins, the flagellar type III export apparatus components FliO, FliP, FliQ, FliR, FlhA, and FlhB, and the substrate specificity switch regulator FliK.

Bacterial transcription is initiated when RNA polymerase is directed to specific promoter sequences by the action of the sigma subunit (1). All bacteria encode a highly conserved ubiquitous σ^A/σ^{70} class sigma factor for generalized, vegetative, and housekeeping gene expression. For specialized gene expression, however, many bacteria also encode alternative sigma factors that differentially control regulons of genes in response to physiological or environmental conditions such as nutrient starvation, heat shock, envelope stress, and motility (2). One way to conditionally restrict alternative sigma factor activity is by production of an anti-sigma factor that binds to, and directly antagonizes, its cognate sigma factor (3). One of the better-understood examples of alternative sigma factor regulon control is that of an alternative sigma factor governing flagellar assembly, σ^{28}, by its anti-sigma factor, FlgM (4).

Flagella are constructed from over 20 different proteins that must be assembled in the correct order and in the correct stoichiometry (5). To ensure proper assembly, flagellar gene expression is organized in at least two hierarchical levels defined here as "early-class" genes, recognized by σ^{70}, and "late-class" genes, recognized by the alternative sigma factor σ^{28} (6). Early-class flagellar genes encode the flagellar type III export apparatus, the structural components of the hook-basal body, and the alternative sigma factor σ^{28}, which is held inactive through direct protein interaction with its cognate anti-sigma factor, FlgM (Fig. 1A) (7–9). Flagella are assembled in part by type III secretion, and when the hook-basal body is complete, the regulator FliK instructs the secretion apparatus to change specificity to recognize and secrete late-class flagellar proteins (10–12), including the anti-sigma factor FlgM (Fig. 1B) (13, 14). FlgM secretion liberates its cognate, σ^{28}, to direct expression of the late-class flagellar genes, such as the gene that encodes the flagellar filament structural protein, flagellin (Fig. 1C) (8, 15). Thus, completion of an assembly intermediate (the hook-basal body) permits the expression of late-class flagellar genes by controlling secretion of an anti-sigma factor. The FlgM secretion model of morphogenetic coupling of flagellar structure and regulation was established in the Gram-negative bacterium *Salmonella enterica* but has not been supported outside the gammaproteobacteria (16).

The Gram-positive bacterium *Bacillus subtilis* synthesizes flagella and encodes both a homolog of the σ^{28} alternative sigma factor, σ^D, and FlgM (17–19). The early-class genes are organized in a long, 32-gene, 27-kb operon called the *fla-che* operon, which is primarily expressed from a σ^A-dependent promoter (20–23). The late-class flagellar genes are σ^D dependent and part of a large regulon that also includes cell-separating peptidoglycan hydrolases (24–28). Mutation of certain genes in the *fla-che* operon required for hook-basal body assembly has been shown to abolish σ^D-dependent gene expression and cause cells both to lose motility and to grow in long chains (20, 21, 29). Furthermore, mutation of FlgM has been shown to restore σ^D-dependent gene expression in these mutants (18, 30–33) suggesting that, like in *S. enterica*, an incomplete hook-basal body antagonizes FlgM function. Unlike what has been reported for *S. enterica*, however, secretion of *B. subtilis* FlgM has never been shown, and thus the mechanism of FlgM inhibition has remained unknown.

Here we show that *B. subtilis* FlgM is secreted by the flagellar export apparatus, consistent with the model of morphogenetic coupling proposed in *S. enterica* (Fig. 1B). Once secreted, FlgM is degraded by extracellular proteases, and we propose that FlgM proteolysis likely prohibited detection of FlgM secretion previously (Fig. 1D). By mutating every gene in the *fla-che* operon, we found that FlgM secretion and σ^D activation were tightly correlated (Fig. 1E). Finally, by overriding native regulation, we identify a minimal core subset of flagellar proteins required for FlgM secretion, including six genes for the flagellar type III export appa-

Received 17 September 2014 **Accepted** 7 October 2014

Accepted manuscript posted online 13 October 2014

Citation Calvo RA, Kearns DB. 2015. FlgM is secreted by the flagellar export apparatus in *Bacillus subtilis*. J Bacteriol 197:81–91. doi:10.1128/JB.02324-14.

Editor: G. A. O'Toole

Address correspondence to Daniel B. Kearns, dbkearns@indiana.edu.

Supplemental material for this article may be found at http://dx.doi.org/10.1128/JB.02324-14.

doi:10.1128/JB.02324-14

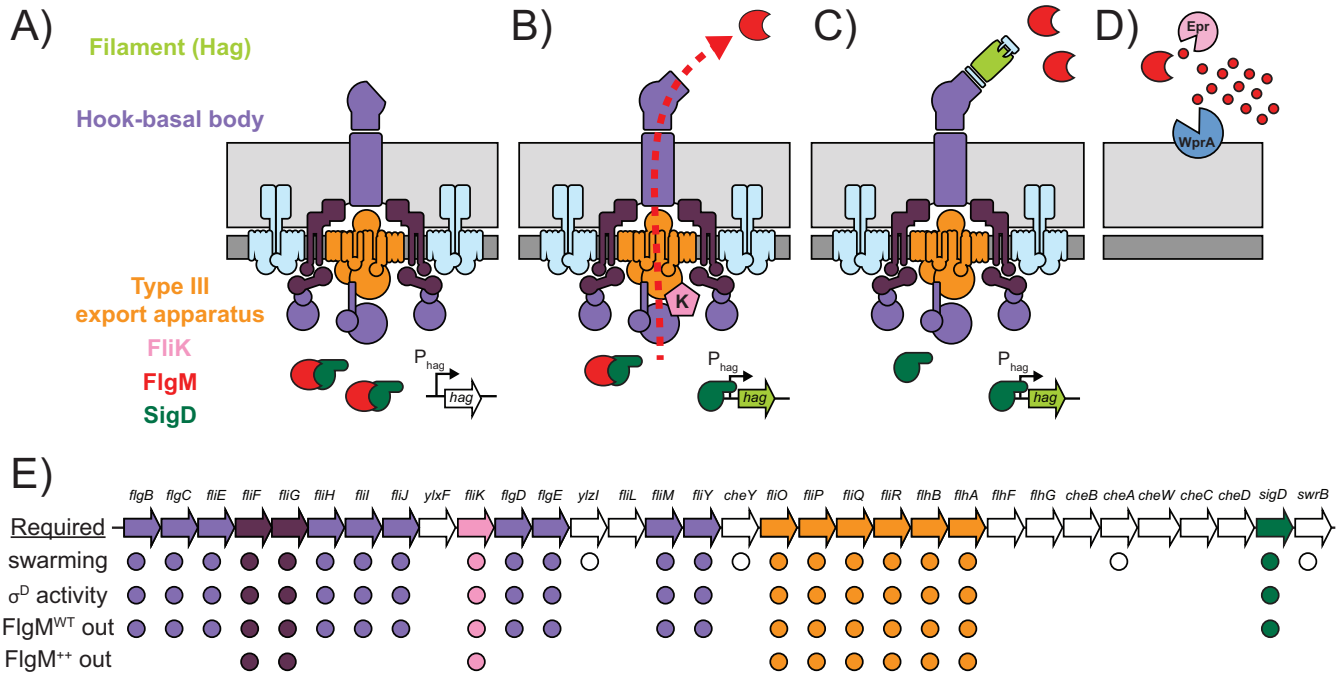

FIG 1 Model for FlgM regulation. (A to C) Extrapolation of the *S. enterica* model for FlgM inhibition as it might function for a Gram-positive organism. (A) Prior to hook-basal body completion (purple), FlgM (red) binds to and inhibits σ^D (dark green) intracellularly. (B) Upon hook-basal body completion, FliK (pink) changes the secretion specificity of the flagellar type III export apparatus (orange) to recognize and secrete FlgM. (C) Liberated σ^D directs transcription of the σ^D regulon, including the *hag* gene (light green), encoding the flagellar filament protein Hag. (D) In *B. subtilis*, extracellular FlgM is proteolyzed by the activity of two proteases, Epr and WprA. Light gray represents peptidoglycan, and dark gray represents cytoplasmic membrane. (E) Cartoon diagram of the *fla-che* operon. Genes predicted to encode flagellar structural proteins are colored purple, and genes predicted to encode type III export apparatus components are colored orange. For each phenotype examined in the study, i.e., swarming motility (migration over 0.7% LB agar), σ^D activity (expression of P_{hag}-GFP), $FlgM^{WT}$ out (secretion of FlgM expressed from its native promoter), and $FlgM^{++}$ out (secretion of FlgM expressed from an IPTG-inducible promoter), a circle is indicated below the gene if that gene product was found to be essential for the respective phenotype. Thus, purple circles indicate hook-basal body structural proteins, white circles indicate nonstructural proteins, and orange circles indicate type III export apparatus homologs required for the indicated phenotype. Green circles indicate *sigD*, and pink circles indicate *fliK*.

ratus, the FliF and FliG basal body components, and the substrate specificity switch protein FliK.

MATERIALS AND METHODS

Strains and growth conditions. *B. subtilis* strains were grown in Luria-Bertani (LB) (10 g tryptone, 5 g yeast extract, 5 g NaCl per liter) broth or on LB plates fortified with 1.5% Bacto agar at 37°C. When appropriate, antibiotics were included at the following concentrations: 10 μg/ml tetracycline (Tet), 100 μg/ml spectinomycin (Spc), 5 μg/ml chloramphenicol (Cat), 5 μg/ml kanamycin (Kan), and 1 μg/ml erythromycin plus 25 μg/ml lincomycin (Mls). IPTG (isopropyl β-D-thiogalactopyranoside; Sigma) was added to the medium at the indicated concentration when appropriate.

Strain construction. Constructs were introduced into the PY79 or DS2569 strain background using DNA transformation and were then transferred to wild-type (WT) strain 3610 using SPP1-mediated generalized phage transduction (34). All strains are in the 3610 background unless otherwise noted. Strains used in this study are listed in Table 1. Plasmids used in this study are listed in Table S1 in the supplemental material. Primers used in this study are listed in Table S2 in the supplemental material.

(i) In-frame deletions. To build the integrative in-frame deletion plasmids, one ~500-bp fragment upstream and one ~500-bp fragment downstream of the gene of interest were PCR amplified, digested with the appropriate restriction endonucleases, and cloned into pMiniMad (35). DNA amplicons were designed such that they removed a portion of the coding sequence of the gene of interest without disrupting the reading frame.

Plasmid DNA purified from *Escherichia coli* TG1was introduced into strain DS2569 by single-crossover integration using transformation at the restrictive temperature for plasmid replication (37°C) and Mls resistance as a selection. The integrated plasmid was then transduced into 3610. To evict the plasmid, the strain was grown overnight (~14 h) in 3 ml LB broth at a permissive temperature for plasmid replication (22°C) and then serially diluted and plated on LB agar plates at 37°C. Individual colonies were patched onto LB plates and LB plates containing Mls to identify Mls-sensitive colonies that had evicted the plasmid. Chromosomal DNA from colonies that had excised the plasmid was purified and screened by PCR using appropriate primers to determine which isolate retained the in-frame deletion allele.

***(a)* Δ7 protease mutant.** The *aprE* deletion plasmid pDP314 was built using primer pairs 1751/1752 and 1753/1754. The *aprE* deletion was resolved in DS2569 to generate strain DS5648. The *nprE* deletion plasmid pDP313 was built using primer pairs 1747/1748 and 1749/1750. The *nprE* deletion was resolved in DS5648 to generate strain DS5700. The *bpr* deletion plasmid pDP311 was built using primer pairs 1739/1740 and 1741/1742. The *bpr* deletion was resolved in DS5700 to generate strain DS5771. The *epr* deletion plasmid pDP315 was built using primer pairs 1755/1756 and 1757/1758. The *epr* deletion was resolved in DS5771 to generate strain DS5810. The *vpr* deletion plasmid pDP312 was built using primer 1743/1744 and 1745/1746. The *vpr* deletion was resolved in DS5810 to generate strain DS5893. The *wprA* deletion plasmid pDP317 was built using primer pairs 1763/1764 and 1765/1766. The *wprA* deletion was resolved in DS5893 to generate strain DS6105. The *mpr* deletion plasmid pDP320 was built using primer pairs 1759/1760 and 1761/1762. The *mpr* deletion was

TABLE 1 Strains used in this study

B. subtilis strain	Relevant genotype or description
Parental strains	
3610	Wild type (ancestral strain)
DS2569	Cured strain (3610 lacking pBS32)
DS6329	Δ*aprE* Δ*nprE* Δ*bpr* Δ*epr* Δ*vpr* Δ*wprA* Δ*mpr* (Δ7 protease or Δ7)
PY79	*swrA*^{PY79} *sfp*^{0} (laboratory strain)
Derivative strains	
DK214	Δ*aprE* Δ*nprE* Δ*bpr* Δ*epr wprA*::*cat amyE*::$P_{hyspank}$-*flgM* Spc^r
DK215	Δ*aprE* Δ*nprE* Δ*bpr wprA*::*cat amyE*::$P_{hyspank}$-*flgM* Spc^r
DK216	Δ*aprE* Δ*nprE wprA*::*cat amyE*::$P_{hyspank}$-*flgM* Spc^r
DK217	Δ*aprE wprA*::*cat amyE*::$P_{hyspank}$-*flgM* Spc^r
DK382	*wprA*::*cat*
DK383	*epr*::*kan*
DK462	*wprA*::*cat epr*::*kan*
DK717	Δ7 Δ*flgB*
DK1142	Δ7 Δ*flhA amyE*::$P_{hyspank}$-*flgM* Spc^r
DK1143	Δ7 Δ*flgC amyE*::$P_{hyspank}$-*flgM* Spc^r
DK1144	Δ7 Δ*flgE amyE*::$P_{hyspank}$-*flgM* Spc^r
DK1856	Δ*flgB flgM*::*tet amyE*::P_{hag}-GFP Cat^{rr}
DK1857	Δ*flgC flgM*::*tet amyE*::P_{hag}-GFP Cat^{rr}
DK1858	Δ*fliE flgM*::*tet amyE*::P_{hag}-GFP Cat^{rr}
DK1859	Δ*fliG flgM*::*tet amyE*::P_{hag}-GFP Cat^{rr}
DK1860	Δ*fliH flgM*::*tet amyE*::P_{hag}-GFP Cat^{rr}
DK1861	Δ*fliI flgM*::*tet amyE*::P_{hag}-GFP Cat^{rr}
DK1862	Δ*fliJ flgM*::*tet amyE*::P_{hag}-GFP Cat^{rr}
DK1863	Δ*ylxF flgM*::*tet amyE*::P_{hag}-GFP Cat^{rr}
DK1864	Δ*fliK flgM*::*tet amyE*::P_{hag}-GFP Cat^{rr}
DK1865	Δ*flgD flgM*::*tet amyE*::P_{hag}-GFP Cat^{rr}
DK1866	Δ*flgE flgM*::*tet amyE*::P_{hag}-GFP Cat^{rr}
DK1867	Δ*ylzI flgM*::*tet amyE*::P_{hag}-GFP Cat^{r}
DK1868	Δ*fliL flgM*::*tet amyE*::P_{hag}-GFP Cat^{r}
DK1869	Δ*fliM flgM*::*tet amyE*::P_{hag}-GFP Cat^{r}
DK1870	Δ*fliY flgM*::*tet amyE*::P_{hag}-GFP Cat^{r}
DK1871	Δ*cheY flgM*::*tet amyE*::P_{hag}-GFP Cat^{r}
DK1872	Δ*fliO flgM*::*tet amyE*::P_{hag}-GFP Cat^{r}
DK1873	Δ*fliP flgM*::*tet amyE*::P_{hag}-GFP Cat^{r}
DK1874	Δ*fliQ flgM*::*tet amyE*::P_{hag}-GFP Cat^{r}
DK1875	Δ*fliR flgM*::*tet amyE*::P_{hag}-GFP Cat^{r}
DK1876	Δ*flhB flgM*::*tet amyE*::P_{hag}-GFP Cat^{r}
DK1877	Δ*flhA flgM*::*tet amyE*::P_{hag}-GFP Cat^{r}
DK1878	Δ*flhF flgM*::*tet amyE*::P_{hag}-GFP Cat^{r}
DK1879	Δ*flhG flgM*::*tet amyE*::P_{hag}-GFP Cat^{r}
DK1880	Δ*cheB flgM*::*tet amyE*::P_{hag}-GFP Cat^{r}
DK1881	Δ*cheA flgM*::*tet amyE*::P_{hag}-GFP Cat^{r}
DK1882	Δ*cheW flgM*::*tet amyE*::P_{hag}-GFP Cat^{r}
DK1883	Δ*cheC flgM*::*tet amyE*::P_{hag}-GFP Cat^{r}
DK1884	Δ*cheD flgM*::*tet amyE*::P_{hag}-GFP Cat^{r}
DK1885	Δ*sigD flgM*::*tet amyE*::P_{hag}-GFP Cat^{r}
DK1886	Δ*swrB flgM*::*tet amyE*::P_{hag}-GFP Cat^{r}
DK1902	Δ7 Δ*fliG*
DK1903	Δ7 Δ*fliQ*
DK1904	Δ7 Δ*fliY*
DK1935	Δ7 Δ*comI*
DK1951	Δ7 Δ*comI* Δ*fliH*
DK1952	Δ7 Δ*comI* Δ*fliJ*
DK1953	Δ7 Δ*comI* Δ*fliM*
DK1968	Δ7 Δ*comI* Δ*flhB*
DK1969	Δ7 Δ*comI* Δ*fliO*
DK1970	Δ7 Δ*comI* Δ*flgD*
DK1971	Δ7 Δ*comI* Δ*fliK*
DK2012	Δ7 Δ*comI* Δ*fliE*
DK2013	Δ7 Δ*comI* Δ*cheA*
DK2014	Δ7 Δ*comI* Δ*ylzI*
DK2026	Δ7 Δ*comI* Δ*ylxF*
DK2027	Δ7 Δ*comI* Δ*cheC*
DK2028	Δ7 Δ*comI* Δ*fliL*
DK2029	Δ7 Δ*comI* Δ*cheD*
DK2030	Δ7 Δ*comI* Δ*cheW*
DK2031	Δ7 Δ*comI* Δ*cheY*
DK2058	Δ7 Δ*comI* Δ*fliI*
DK2059	Δ7 Δ*comI* Δ*fliP*
DK2060	Δ7 Δ*comI* Δ*cheB*
DK2071	Δ7 Δ*comI* Δ*flhG*
DK2230	Δ7 Δ*comI* Δ*sigD*
DK2301	Δ7 Δ*comI* Δ*sigD amyE*::$P_{hyspank}$-*flgM* Spc^r
DK3051	Δ7 Δ*flgB amyE*::$P_{hyspank}$-*flgM* Spc^r
DK3052	Δ7 Δ*comI* Δ*fliH amyE*::$P_{hyspank}$-*flgM* Spc^r
DK3053	Δ7 Δ*comI* Δ*fliE amyE*::$P_{hyspank}$-*flgM* Spc^r
DK3054	Δ7 Δ*fliG amyE*::$P_{hyspank}$-*flgM* Spc^r
DK3055	Δ7 Δ*comI* Δ*fliI amyE*::$P_{hyspank}$-*flgM* Spc^r
DK3056	Δ7 Δ*comI* Δ*fliJ amyE*::$P_{hyspank}$-*flgM* Spc^r
DK3057	Δ7 Δ*comI* Δ*ylxF amyE*::$P_{hyspank}$-*flgM* Spc^r
DK3058	Δ7 Δ*comI* Δ*fliK amyE*::$P_{hyspank}$-*flgM* Spc^r
DK3059	Δ7 Δ*comI* Δ*flgD amyE*::$P_{hyspank}$-*flgM* Spc^r
DK3060	Δ7 Δ*comI* Δ*ylzI amyE*::$P_{hyspank}$-*flgM* Spc^r
DK3061	Δ7 Δ*comI* Δ*fliL amyE*::$P_{hyspank}$-*flgM* Spc^r
DK3062	Δ7 Δ*comI* Δ*fliM amyE*::$P_{hyspank}$-*flgM* Spc^r
DK3063	Δ7 Δ*fliY amyE*::$P_{hyspank}$-*flgM* Spc^r
DK3064	Δ7 Δ*comI* Δ*cheY amyE*::$P_{hyspank}$-*flgM* Spc^r
DK3065	Δ7 Δ*comI* Δ*fliO amyE*::$P_{hyspank}$-*flgM* Spc^r
DK3066	Δ7 Δ*comI* Δ*fliP amyE*::$P_{hyspank}$-*flgM* Spc^r
DK3067	Δ7 Δ*fliQ amyE*::$P_{hyspank}$-*flgM* Spc^r
DK3068	Δ7 Δ*comI* Δ*flhB amyE*::$P_{hyspank}$-*flgM* Spc^r
DK3069	Δ7 Δ*comI* Δ*flhG amyE*::$P_{hyspank}$-*flgM* Spc^r
DK3070	Δ7 Δ*comI* Δ*cheB amyE*::$P_{hyspank}$-*flgM* Spc^r
DK3071	Δ7 Δ*comI* Δ*cheA amyE*::$P_{hyspank}$-*flgM* Spc^r
DK3072	Δ7 Δ*comI* Δ*cheW amyE*::$P_{hyspank}$-*flgM* Spc^r
DK3073	Δ7 Δ*comI* Δ*cheC amyE*::$P_{hyspank}$-*flgM* Spc^r
DK3074	Δ7 Δ*comI* Δ*cheD amyE*::$P_{hyspank}$-*flgM* Spc^r
DK3075	Δ7 Δ*comI* Δ*swrB*
DK3076	Δ7 Δ*comI* Δ*fliR*
DK3077	Δ7 Δ*comI* Δ*flhF*
DK3078	Δ7 Δ*comI* Δ*swrB amyE*::$P_{hyspank}$-*flgM* Spc^r
DK3079	Δ7 Δ*comI* Δ*fliR amyE*::$P_{hyspank}$-*flgM* Spc^r
DK3080	Δ7 Δ*comI* Δ*flhF amyE*::$P_{hyspank}$-*flgM* Spc^r
DS908	*amyE*::P_{hag}-GFP Cat^r
DS2509	Δ*swrB*
DS3772	*amyE*::$P_{hyspank}$-*flgM* Spc^r
DS4029	Δ*flgM*
DS4264	*flgM*::*tet amyE*::P_{hag}-GFP Cat^r
DS4536	Δ*fliK*
DS4680	Δ*flgB*
DS4681	Δ*flgE*
DS5384	Δ*fliY*
DS5648	Δ*aprE*
DS5700	Δ*aprE* Δ*nprE*
DS5771	Δ*aprE* Δ*nprE* Δ*bpr*
DS5810	Δ*aprE* Δ*nprE* Δ*bpr* Δ*epr*
DS5893	Δ*aprE* Δ*nprE* Δ*bpr* Δ*epr* Δ*vpr*
DS5913	Δ*flhA*

(Continued on following page)

TABLE 1 (Continued)

B. subtilis strain	Relevant genotype or description
DS6105	Δ*aprE* Δ*nprE* Δ*bpr* Δ*epr* Δ*vpr* Δ*wprA*
DS6420	Δ*sigD*
DS6468	Δ*fliO*
DS6540	Δ*fliL*
DS6554	Δ*ylxF*
DS6555	Δ*flgD*
DS6657	Δ*ylzI*
DS6658	Δ*flhF*
DS6728	Δ*fliI*
DS6729	Δ*fliH*
DS6775	Δ*fliM*
DS6806	Δ7 *amyE*::$P_{hyspank}$-*flgM* Spc^r
DS6867	Δ*cheC*
DS6868	Δ*cheD*
DS6869	Δ*cheW*
DS6870	Δ*cheY*
DS6871	Δ7 Δ*fliF*
DS6887	Δ*cheA*
DS6919	Δ7 Δ*fliF amyE*::$P_{hyspank}$-*flgM* Spc^r
DS7080	Δ*fliF*
DS7118	Δ*fliQ*
DS7119	Δ*fliP*
DS7120	Δ*flhB*
DS7161	Δ7 Δ*flgM*
DS7303	Δ*flgC*
DS7306	Δ*cheB*
DS7308	Δ*fliE*
DS7317	Δ*fliR*
DS7357	Δ*fliG*
DS7358	Δ*flhG*
DS7359	Δ*fliJ*
DS7457	Δ*fliF flgM*::*tet amyE*::P_{hag}-GFP Cat^r
DS7684	Δ*flgB amyE*::P_{hag}-GFP Cat^r
DS7685	Δ*flgC amyE*::P_{hag}-GFP Cat^r
DS7686	Δ*fliE amyE*::P_{hag}-GFP Cat^r
DS7687	Δ*fliF amyE*::P_{hag}-GFP Cat^r
DS7688	Δ*fliG amyE*::P_{hag}-GFP Cat^r
DS7689	Δ*fliH amyE*::P_{hag}-GFP Cat^r
DS7690	Δ*fliI amyE*::P_{hag}-GFP Cat^r
DS7691	Δ*fliJ amyE*::P_{hag}-GFP Cat^r
DS7692	Δ*ylxF amyE*::P_{hag}-GFP Cat^r
DS7693	Δ*fliK amyE*::P_{hag}-GFP Cat^r
DS7694	Δ*flgD amyE*::P_{hag}-GFP Cat^r
DS7695	Δ*flgE amyE*::P_{hag}-GFP Cat^r
DS7696	Δ*ylzI amyE*::P_{hag}-GFP Cat^r
DS7697	Δ*fliL amyE*::P_{hag}-GFP Cat^r
DS7698	Δ*fliM amyE*::P_{hag}-GFP Cat^r
DS7699	Δ*fliY amyE*::P_{hag}-GFP Cat^r
DS7700	Δ*cheY amyE*::P_{hag}-GFP Cat^r
DS7701	Δ*fliO amyE*::P_{hag}-GFP Cat^r
DS7702	Δ*fliP amyE*::P_{hag}-GFP Cat^r
DS7703	Δ*fliQ amyE*::P_{hag}-GFP Cat^r
DS7704	Δ*fliR amyE*::P_{hag}-GFP Cat^r
DS7705	Δ*flhB amyE*::P_{hag}-GFP Cat^r
DS7706	Δ*flhA amyE*::P_{hag}-GFP Cat^r
DS7707	Δ*flhF amyE*::P_{hag}-GFP Cat^r
DS7708	Δ*flhG amyE*::P_{hag}-GFP Cat^r
DS7709	Δ*cheB amyE*::P_{hag}-GFP Cat^r
DS7710	Δ*cheA amyE*::P_{hag}-GFP Cat^r
DS7711	Δ*cheW amyE*::P_{hag}-GFP Cat^r
DS7712	Δ*cheC amyE*::P_{hag}-GFP Cat^r

TABLE 1 (Continued)

B. subtilis strain	Relevant genotype or description
DS7713	Δ*cheD amyE*::P_{hag}-GFP Cat^r
DS7714	Δ*sigD amyE*::P_{hag}-GFP Cat^r
DS7715	Δ*swrB amyE*::P_{hag}-GFP Cat^r
DS8080	Δ*aprE* Δ*nprE* Δ*bpr* Δ*epr* Δ*vpr* Δ*wprA amyE*::$P_{hyspank}$-*flgM* Spc^r
DS8081	Δ*aprE* Δ*nprE* Δ*bpr* Δ*epr* Δ*vpr amyE*::$P_{hyspank}$-*flgM* Spc^r
DS8082	Δ*aprE* Δ*nprE* Δ*bpr* Δ*epr amyE*::$P_{hyspank}$-*flgM* Spc^r
DS8083	Δ*aprE* Δ*nprE* Δ*bpr amyE*::$P_{hyspank}$-*flgM* Spc^r
DS8084	Δ*aprE* Δ*nprE amyE*::$P_{hyspank}$-*flgM* Spc^r
DS8085	Δ*aprE amyE*::$P_{hyspank}$-*flgM* Spc^r
DS8117	Δ7 Δ*flhA*
DS8365	Δ7 Δ*flgE*
DS8404	Δ7 Δ*flgC*

resolved in DS6105 to generate strain DS6329, the Δ7 protease mutant strain.

***(b) fla-che* operon gene deletions.** The *flgB* deletion plasmid pDP305 was built using primer pairs 1479/1480 and 1481/1482. The *flgC* deletion plasmid pDP349 was built using primer pairs 2317/2318 and 2319/2320. The *fliE* deletion plasmid pDP350 was built using primer pairs 2321/2322 and 2323/2324. The *fliF* deletion plasmid pLC16 was built using primer pairs 1900/1901 and 1898/1899. The *fliG* deletion plasmid pKB40 was built using primer pairs 770/771 and 772/773. The *fliH* deletion plasmid pDP335 was built using primer pairs 2122/2123 and 2124/2125. The *fliI* deletion plasmid pDP336 was built using primer pairs 2126/2127 and 2128/2129. The *fliJ* deletion plasmid pLC25 was built using primer pairs 857/858 and 859/860. The *ylxF* deletion plasmid pDP327 was built using primer pairs 2029/2030 and 2031/2032. The *fliK* deletion plasmid pKB93 was built using primer pairs 1387/1388 and 1389/1390. The *flgD* deletion plasmid pDP328 was built using primer pairs 2033/2034 and 2035/2036. The *flgE* deletion plasmid pDP306 was built using primer pairs 1483/1484 and 1485/1486. The *ylzI* deletion plasmid pDP329 was built using primer pairs 2037/2038 and 2039/2040. The *fliL* deletion plasmid pDP330 was built using primer pairs 2041/2042 and 2043/2044. The *fliM* deletion plasmid pSG32 was built using primer pairs 1569/1570 and 1571/1572. The *fliY* deletion plasmid pSG6 was built using primer pairs 1574/1575 and 1576/1577. The *cheY* deletion plasmid pDP343 was built using primer pairs 2197/2198 and 2199/2200. The *fliO* deletion plasmid pDP332 was built using primer pairs 1692/1693 and 1694/1695. The *fliP* deletion plasmid pDP346 was built using primer pairs 2290/2291 and 2292/2293. The *fliQ* deletion plasmid pDP345 was built using primer pairs 2286/2287 and 2288/2289. The *fliR* deletion plasmid pDP351 was built using primer pairs 2325/2326 and 2327/2328. The *flhB* deletion plasmid pDP347 was built using primer pairs 2294/2295 and 2296/2297. The *flhA* deletion plasmid pLC47 was built using primer pairs 976/977 and 978/979. The *flhF* deletion plasmid pDP333 was built using primer pairs 2103/2104 and 2105/2106. The *flhG* deletion plasmid pLC22 was built using primer pairs 826/827 and 828/829. The *cheB* deletion plasmid pDP344 was built using primer pairs 2282/2283 and 2284/2285. The *cheA* deletion plasmid pDP338 was built using primer pairs 2177/2178 and 2179/2180. The *cheW* deletion plasmid pDP342 was built using primer pairs 2193/2194 and 2195/2196. The *cheC* deletion plasmid pDP340 was built using primer pairs 2185/2186 and 2187/2188. The *cheD* deletion plasmid pDP341 was built using primer pairs 2189/2190 and 2191/2192. The *sigD* deletion plasmid pDP326 was built using primer pairs 2019/2020 and 2021/2022. The *swrB* deletion plasmid pDP242 was built using primer pairs 740/741 and 839/840. The *swrB* deletion plasmid pRC62 was built using primer pairs 4190/4191 and 4192/4193.

***(c) fla-che* operon gene deletions in Δ7 protease mutant background.** To generate the Δ7 protease Δ*comI* mutant, the in-frame markerless deletion construct pMP50 was introduced into the Δ7 protease

mutant background by SPP1-mediated generalized transduction. The *comI* gene was deleted as previously described to generate DK1935. Each *fla-che* gene deletion construct purified from *E. coli* TG1 was transformed into DK1935 and deleted as previously described. For certain *fla-che* gene deletions, SPP1-mediated generalized transduction was successfully used to introduce the deletion constructs directly into the Δ7 protease mutant background (Table 1).

(ii) Δ*flgM*::*tet*. The Δ*flgM*::*tet* insertion-deletion allele was generated by long flanking homology PCR (using primer pairs 140/141 and 142/143), and DNA containing a tetracycline drug resistance gene (pDG1515) was used as a template for marker replacement (36).

(iii) Δ*wprA*::*cat*. The Δ*wprA*::*cat* insertion-deletion allele was generated by long flanking homology PCR (using primer pairs 3260/3261 and 3262/3263), and DNA containing a chloramphenicol resistance gene (pAC225) was used as a template for marker replacement (pAC225 was a generous gift from Amy Camp, Mount Holyoke College).

(iv) Δ*epr*::*kan*. The Δ*epr*::*kan* insertion-deletion allele was generated by long flanking homology PCR (using primer pairs 721/722 and 723/724), and DNA containing a kanamycin resistance gene (pDG780) was used as a template for marker replacement (36).

(v) Inducible constructs. To generate the inducible *amyE*::$P_{hyspank}$-*flgM* Spc overexpression construct pRC21, a fragment containing the *flgM* gene was PCR amplified using primer pair 3330/1135 and 3610 genomic DNA as a template. The resulting PCR product was digested with NheI and SphI and ligated into the NheI and SphI sites of pDR111 containing a spectinomycin resistance cassette, a polylinker downstream of the $P_{hyspank}$ promoter, and the gene encoding the LacI repressor between the arms of the *amyE* gene (37).

(vi) 6His-SUMO-FlgM protein expression constructs. To generate the translational fusion of FlgM to the 6His-SUMO tag, a fragment containing *flgM* was PCR amplified using strain 3610 DNA as a template and primer pair 933/934 and was digested with SapI and XhoI. The fragment was ligated into the SapI and XhoI sites of plasmid pTB146 containing an ampicillin resistance cassette to create pDP266 (38).

SPP1 phage transduction. To 0.2 ml of dense culture grown in TY broth (LB broth supplemented after autoclaving with 10 mM $MgSO_4$ and 100 μM $MnSO_4$), serial dilutions of SPP1 phage stock were added and statically incubated for 15 min at 37°C. To each mixture, 3 ml TYSA (molten TY supplemented with 0.5% agar) was added, poured atop fresh TY plates, and incubated at 30°C overnight. Top agar from the plate containing near-confluent plaques was harvested by scraping into a 15-ml conical tube, vortexed, and centrifuged at 5,000 × *g* for 10 min. The supernatant was treated with 25 μg/ml DNase (final concentration) before being passed through a 0.45-μm syringe filter and stored at 4°C.

Recipient cells were grown to stationary phase in 2 ml TY broth at 37°C. One milliliter of cells was mixed with 25 μl of SPP1 donor phage stock. Nine milliliters of TY broth was added to the mixture and allowed to mix by gentle rocking at 25°C for 30 min. The transduction mixture was then centrifuged at 5,000 × *g* for 10 min, the supernatant was discarded, and the pellet was resuspended in the residual volume. One hundred microliters of cell suspension was then plated on LB fortified with 1.5% agar, the appropriate antibiotic, and 10 mM sodium citrate.

Swarm expansion assay. Cells were grown to mid-log phase at 37°C in LB broth and resuspended to an optical density at 600 nm (OD_{600}) of 10 in pH 8.0 phosphate-buffered saline (PBS) buffer (137 mM NaCl, 2.7 mM KCl, 10 mM Na_2HPO_4, and 2 mM KH_2PO_4) containing 0.5% India ink (Higgins). Freshly prepared LB containing 0.7% Bacto agar (25 ml/plate) was dried for 20 min in a laminar flow hood, centrally inoculated with 10 μl of the cell suspension, dried for another 10 min, and incubated at 37°C. After 5 h, the radius of swarm expansion was measured and recorded for each strain.

Microscopy. Fluorescence microscopy was performed with a Nikon 80i microscope with a phase-contrast objective Nikon Plan Apo 100X and an Excite 120 metal halide lamp. FM4-64 was visualized with a C-FL HYQ Texas Red filter cube (excitation filter, 532 to 587 nm; barrier filter, >590 nm). Green fluorescent protein (GFP) was visualized using a C-FL HYQ fluorescein isothiocyanate (FITC) filter cube (for FITC, excitation filter, 460 to 500 nm, and barrier filter, 515 to 550 nm). Images were captured with a Photometrics Coolsnap HQ2 camera in black and white, false colored, and superimposed using Metamorph image software.

For GFP fluorescence microscopy, cells were grown to mid-log phase (OD_{600}, 0.4 to 0.9) in 2 ml of LB broth at 37°C, and 1 ml was pelleted and washed with 1 ml PBS. Membranes were stained by resuspending the cell pellet in 50 μl of PBS containing 5 μg/ml FM4-64 and incubated for 5 min at room temperature in the dark. Samples were observed by spotting 3 μl of the suspension on a glass microscope slide and were immobilized with a poly-L-lysine-treated coverslip.

FlgM protein purification. The 6His-SUMO-FlgM fusion protein expression vector pDP266 was transformed into Rosetta-gami II *E. coli*, and the resulting strain was grown to an OD_{600} of ~0.8 at 37°C with shaking in 1 liter of Terrific Broth supplemented with 100 μg/ml ampicillin (12 g tryptone, 25 g yeast extract, 0.4% glycerol per 900 ml, with addition of 100 ml sterile potassium phosphate solution [2.31 g KH_2PO_4, 12.54 g K_2HPO_4] after autoclaving). Protein expression was induced with the addition of 0.1 mM IPTG, and growth was continued overnight at 16°C. Cells were pelleted, resuspended in lysis/binding buffer (50 mM Na_2HPO_4, 500 mM NaCl, 20 mM imidazole, 0.1 mM phenylmethylsulfonyl fluoride [PMSF]; pH 8.0), and lysed by sonication. Lysed cells were centrifuged at 8,000 × *g* for 30 min at 4°C. Cleared supernatant was combined with 1 ml of nickel-nitrilotriacetic acid (Ni-NTA) His Bind resin (Novagen) equilibrated in lysis/binding buffer and incubated overnight with gentle rotation at 4°C. The resin-lysate mixture was poured into a 1-cm separation column (Bio-Rad), the resin was allowed to pack, and the lysate was allowed to flow through the column. The resin was washed with wash buffer (50 mM Na_2HPO_4, 500 mM NaCl, 40 mM imidazole, 0.1 mM PMSF; pH 8.0). The 6His-SUMO-FlgM fusion protein bound to the resin was eluted using elution buffer (50 mM Na_2HPO_4, 500 mM NaCl, 500 mM imidazole, 0.1 mM PMSF; pH 8.0). Elution products were separated by 15% sodium dodecyl sulfate-polyacrylamide gel electrophoresis (SDS-PAGE) and Coomassie blue stained to verify purification of the 6His-SUMO-FlgM fusion protein and pure fractions.

FlgM antibody production. One milligram of purified 6His-SUMO-FlgM protein was sent to Cocalico Biologicals Inc. for serial injection into a rabbit host for antibody generation. Anti-FlgM serum was mixed with FlgM-conjugated Affigel-10 beads and incubated overnight at 4°C. The beads were packed onto a 1-cm column (Bio-Rad) and then washed with 100 mM glycine (pH 2.5) to release the antibody and immediately neutralized with 2 M Tris base. The purification of the antibody was verified by SDS-PAGE. Purified anti-FlgM antibody was dialyzed into 1× PBS–50% glycerol and stored at −20°C.

FlgM secretion assay. For the pellet fraction (cytoplasmic and cell-associated proteins), *B. subtilis* strains were grown in 25 ml LB broth to an OD_{600} of ~1.0, and 1-ml and 10-ml samples of broth culture were harvested by centrifugation, resuspended to 10 OD_{600} units in lysis buffer (20 mM Tris [pH 7.0], 10 mM EDTA, 1 mg/ml lysozyme, 10 μg/ml DNase I, 100 μg/ml RNase I, 1 mM PMSF), and incubated 30 min at 37°C. For the supernatant fraction (secreted extracellular proteins), 10 ml of supernatant was collected from the same cultures as those used to generate the pellet fractions. The supernatant was clarified by centrifugation at 5,000 × *g* for 30 min and treated with 1 ml of freshly prepared 0.015% sodium deoxycholate for 10 min at room temperature. Proteins from the supernatant were precipitated by adding 500 μl chilled trichloroacetic acid (TCA) and incubating the mixture for >2 h on ice at 4°C. Precipitated proteins were pelleted at 9,447 × *g* for 10 min at 4°C, washed twice with 1 ml ice-cold acetone, and resuspended to 10 OD_{600} units in 0.1 N sodium hydroxide. Ten microliters of cell pellet or supernatant sample was mixed with 2 μl 6× SDS loading buffer. Samples were separated in parallel by 15% SDS-PAGE. Proteins were electroblotted onto nitrocellulose for 50 min at 400 mA and probed with a 1:10,000 dilution of anti-FlgM primary antibody, with a 1:40,000 dilution of anti-SigA primary antibody (a gen-

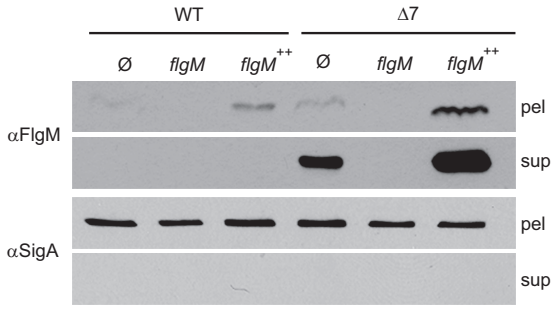

FIG 2 FlgM is secreted and proteolyzed extracellularly. (A) FlgM secretion assay. Cell pellets (pel) were lysed, and supernatants (sup) were concentrated by TCA precipitation of dissolved proteins, resolved by SDS-PAGE, electroblotted, and probed in Western analysis. Anti-FlgM (αFlgM) primary antibody was used to detect FlgM, and anti-SigA (αSigA) served as a loading control and as a control for cytoplasmic contamination of supernatant samples caused by cell lysis. The horizontal bars group strains with the indicated common genetic background. "Ø" indicates no additional change to the genetic background. The following strains were used to generate the figure: 3610 (WT strain), DS4029 (*flgM*), DS3772 (*flgM*$^{++}$), DS6329 (Δ7), DS7161 (Δ7 *flgM*), and DS6806 (Δ7 *flgM*$^{++}$).

erous gift from Masaya Fujita, University of Huston), and with a 1:10,000 dilution of secondary antibody (horseradish peroxidase [HRP]-conjugated goat anti-rabbit immunoglobulin G). Immunoblots were developed using the Pierce ECL Western blotting substrate kit (Thermo Scientific).

RESULTS

FlgM is secreted and degraded extracellularly. FlgM is the anti-sigma factor that inhibits the activity of the motility sigma factor σ^D (19). In *S. enterica*, FlgM activity is inhibited when FlgM is secreted through the flagellar hook-basal body and becomes spatially separated from its cognate sigma factor (13, 14). To test whether FlgM is secreted in *B. subtilis*, Western blot analysis was performed using anti-FlgM primary antibody on TCA-precipitated supernatant and cell pellet lysate fractions of the wild type, an *flgM* mutant, and a strain that expressed *flgM* from the artificial IPTG-inducible $P_{hyspank}$ promoter integrated at the ectopic *amyE* locus (*amyE*::$P_{hyspank}$-*flgM*). In parallel, Western blot assays were conducted using primary antibody against SigA, the constitutive cytoplasmic vegetative sigma factor. SigA serves both as a loading control for cell pellet samples and as a control for cytoplasmic contamination of supernatant samples caused by cell lysis, as SigA is cytoplasmic and is not secreted. FlgM protein was barely detectable in the cell pellet lysates of the wild type, absent from the *flgM* mutant, and enhanced in the $P_{hyspank}$-*flgM* strain when induced with 1 mM IPTG (Fig. 2). Neither FlgM nor SigA was detected in the any of the TCA-precipitated supernatant fractions. We conclude that either FlgM is not secreted in *B. subtilis* or FlgM is secreted and degraded extracellularly.

FlgM could be extracellularly degraded by one or more of the seven extracellular proteases secreted by *B. subtilis*: AprE, NprE, Bpr, Epr, Vpr, WprA, and Mpr (39–45). To test whether extracellular proteases degrade FlgM, a secretion assay was conducted using a mutant containing multiple in-frame markerless deletions disrupting each of the exoprotease-encoding genes ("Δ7 mutant"). In the Δ7 mutant background, FlgM was detected in both the cell pellet lysates and the corresponding TCA-precipitated supernatant fractions from the wild-type and IPTG-induced $P_{hyspank}$-*flgM* strains (Fig. 2). SigA was detected in the cell lysate fraction but was not detected in the TCA-precipitated supernatant fraction, suggesting that SigA was neither secreted nor released by cell lysis. We conclude that FlgM is secreted in *B. subtilis* and that one or more of the seven secreted proteases degraded FlgM in the extracellular environment.

A series of mutants was constructed to reductively deduce which exoprotease(s) contributed to the degradation of FlgM (Fig. 3A). Each strain tested in order lacked a single protease encoded by the preceding strain. Thus, when FlgM was detected in the supernatant, we could infer that the most recently mutated protease contributed to FlgM degradation. FlgM was not detected by

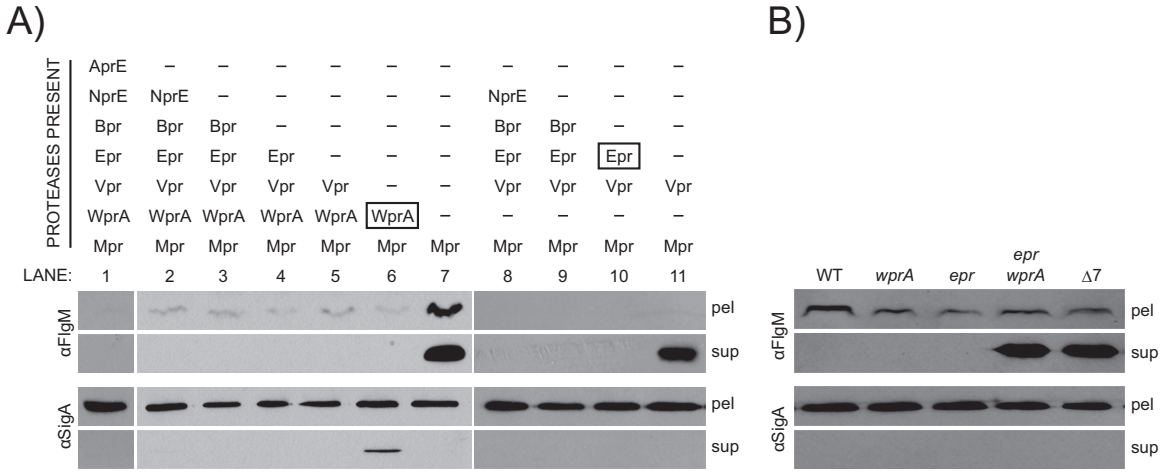

FIG 3 FlgM is specifically proteolyzed by WprA and Epr. (A) FlgM secretion assay. All strains contain the $P_{hyspank}$-*flgM* construct (*flgM*$^{++}$) and were grown in the presence of 1 mM IPTG. Blots were probed with both anti-FlgM (αFlgM) and anti-SigA (αSigA) to serve as a loading and lysis control. The following strains were used to generate the figure: DS6806 (lane 1), DS8085 (lane 2), DS8084 (lane 3), DS8083 (lane 4), DS8082 (lane 5), DS8081 (lane 6), DS8080 (lane 7), DK217 (lane 8), DK216 (lane 9), DK215 (lane 10), and DK214 (lane 11). We note that some SigA was detected in the supernatant of lane 6, presumably due to a low level of spontaneous cell lysis prior to harvesting the supernatant. We further note that the cell lysis that occurred did not seem to contribute significantly to the amount of FlgM in the supernatant. (B) FlgM secretion assay. All strains contain the $P_{hyspank}$-*flgM* construct (*flgM*$^{++}$) and were grown in the presence of 1 mM IPTG. The following strains were used to generate the figure: DS6806 (WT strain), DK382 (*wprA*), DK383 (*epr*), DK462 (*wprA epr*), and DS6329 (Δ7).

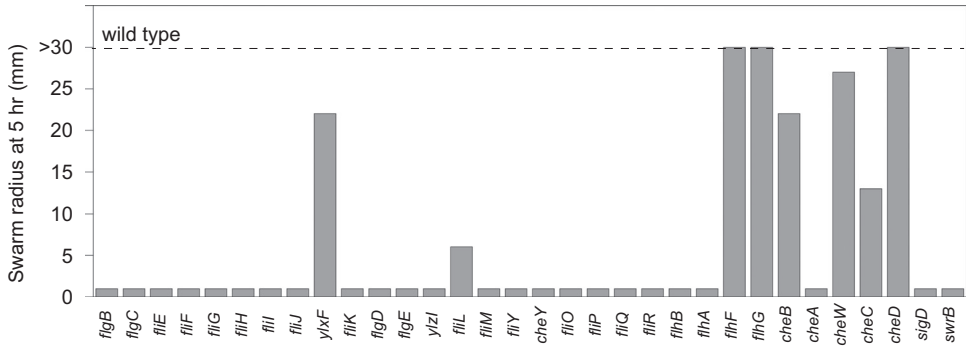

FIG 4 Mutations in the *fla-che* operon abolish swarming motility. Swarm expansion assays were conducted on the indicated strains, and the swarm radius was measured after 5 h of incubation at 37°C. Bars represent averages of three replicates. The dashed line indicates the swarming motility of the wild type (strain 3610) at 5 h. The following strains (mutated genes in parentheses) were used to generate the figure: DS4680 (*flgB*), DS7303 (*flgC*), DS7308 (*fliE*), DS7080 (*fliF*), DS7357 (*fliG*), DS6729 (*fliH*), DS6728 (*fliI*), DS7359 (*fliJ*), DS6554 (*ylxF*), DS4536 (*fliK*), DS6555 (*flgD*), DS4681 (*flgE*), DS6657 (*ylzI*), DS6540 (*fliL*), DS6775 (*fliM*), DS5384 (*fliY*), DS6870 (*cheY*), DS6468 (*fliO*), DS7119 (*fliP*), DS7118 (*fliQ*), DS7317 (*fliR*), DS7120 (*flhB*), DS5913 (*flhA*), DS6658 (*flhF*), DS7358 (*flhG*), DS7306 (*cheB*), DS6887 (*cheA*), DS6869 (*cheW*), DS6867 (*cheC*), DS6868 (*cheD*), DS6420 (*sigD*), and DS2509 (*swrB*).

Western blotting of TCA-precipitated supernatant fractions when strains encoded the exoprotease WprA (Fig. 3A, lane 6) but was detected when WprA was mutated (Fig. 3A, lane 7), suggesting that WprA was involved in FlgM degradation. Mutation of WprA alone, however, was not sufficient to allow for the detection of FlgM in the supernatant fraction, suggesting that one or more of the remaining six exoproteases was also involved (Fig. 3B).

To find additional exoproteases that contributed to FlgM degradation, we reanalyzed a reductive series of exoprotease mutants in which WprA was also mutated. FlgM was not detected in TCA-precipitated supernatants in WprA-mutated strains that encoded the protease Epr (Fig. 3A, lane 10) but was detected when Epr was also mutated, suggesting that Epr contributed to FlgM degradation (Fig. 3A, lane 11). Mutation of Epr alone was also not sufficient to allow for the detection of FlgM in the supernatant fraction, likely due to the presence of WprA (Fig. 3B). Mutation of both WprA and Epr, however, was sufficient to allow for the detection of FlgM in the TCA-precipitated supernatant fraction (Fig. 3B). We conclude that FlgM is proteolytically degraded in the extracellular environment by the combined activity of WprA and Epr. Henceforth, all FlgM secretion assays were conducted in the Δ7 protease mutant background.

FlgM inhibits σ^D activity in flagellar basal body mutants. In *S. enterica*, cells defective in synthesis of the flagellar hook-basal body inhibit σ^{28} activity by an enhanced accumulation of the anti-sigma factor FlgM (7). Thirty-two genes within the *B. subtilis fla-che* operon are predicted to be involved in either flagellar assembly or flagellar function based on their homology to flagellar proteins in *S. enterica* (20). To determine which genes in the *fla-che* operon were required for flagellar assembly and/or function, swarm expansion motility assays were conducted in strains mutated for each of the *fla-che* operon genes (Fig. 4). Mutants able to expand from the point of inoculation after 5 h of incubation were deemed swarming proficient, and based on this criterion, the following genes were considered unlikely candidates essential for the assembly of the hook-basal body: *ylxF*, *fliL*, *flhF*, *flhG*, *cheB*, *cheW*, *cheC*, and *cheD* (Fig. 1E).

In *S. enterica*, defects in flagellar hook-basal body assembly result in the inhibition of σ^{28} activity (7). To determine which mutants in the *fla-che* operon were defective in σ^D activity, a reporter for σ^D-dependent gene expression in which the P_{hag} promoter for the *hag* gene encoding the flagellar filament Hag was transcriptionally fused to green fluorescent protein was integrated at the ectopic *amyE* locus (*amyE*::P_{hag}-GFP) in the wild type and each mutant background (Fig. 5, top left images). Expression of σ^D-dependent genes is heterogenous in the population, and wild-type cells displayed bistable expression of P_{hag}-GFP such that short motile cells were brightly fluorescent and nonmotile chains were dark (28, 46). Mutants that robustly expressed the P_{hag}-GFP reporter did not have a strong defect in σ^D-dependent gene expression, and based on this criterion, the following genes were also considered unlikely candidates essential for the assembly of the hook-basal body: *ylzI*, *cheY*, *cheA*, and *swrB* (Fig. 1E). As further support that *ylzI*, *cheY*, *cheA*, and *swrB* are not essential for hook-basal body assembly, liquid cultures of each mutant exhibited swimming motility when observed in phase-contrast microscopy of wet mounts. In sum, we infer that the following *fla-che*-encoded proteins are required for hook-basal body completion in *B. subtilis*: FlgB, FlgC, FliE, FliF, FliG, FliH, FliI, FliJ, FliK, FlgD, FlgE, FliM, FliY, FliO, FliP, FliQ, FliR, FlhB, and FlhA.

In *S. enterica*, defects in flagellar hook-basal body assembly result in the inhibition of σ^{28} activity due to a failure to inhibit the FlgM anti-sigma factor (7). To determine whether the low fluorescence from the P_{hag}-GFP reporter in the *fla-che* operon mutants was due to enhanced FlgM activity, FlgM was mutated in each *fla-che* operon mutant background (Fig. 5, bottom right images). Mutation of *flgM* increased P_{hag}-GFP fluorescence magnitude in the wild type and was epistatic to all *fla-che* operon mutants irrespective of basal P_{hag}-GFP fluorescence level. We conclude that each of the *fla-che* operon mutants expressing low levels of P_{hag}-GFP experience enhanced inhibition of σ^D-dependent gene expression due to an inability to antagonize FlgM.

FlgM is secreted through the hook-basal body by the flagellar export apparatus. In *S. enterica*, FlgM is inhibited by secretion through a flagellar type III export apparatus that becomes proficient for FlgM secretion only upon completion of the hook-basal body structural intermediate (15). To test whether FlgM secretion depends on a functional hook-basal body in *B. subtilis*, in-frame markerless deletions of each gene in the *fla-che* operon were constructed in the Δ7 protease mutant background. Low levels of FlgM were detected in the cell pellet lysate fraction in each mutant save *sigD*, as *flgM* gene expression is σ^D dependent (Fig. 6A). Im-

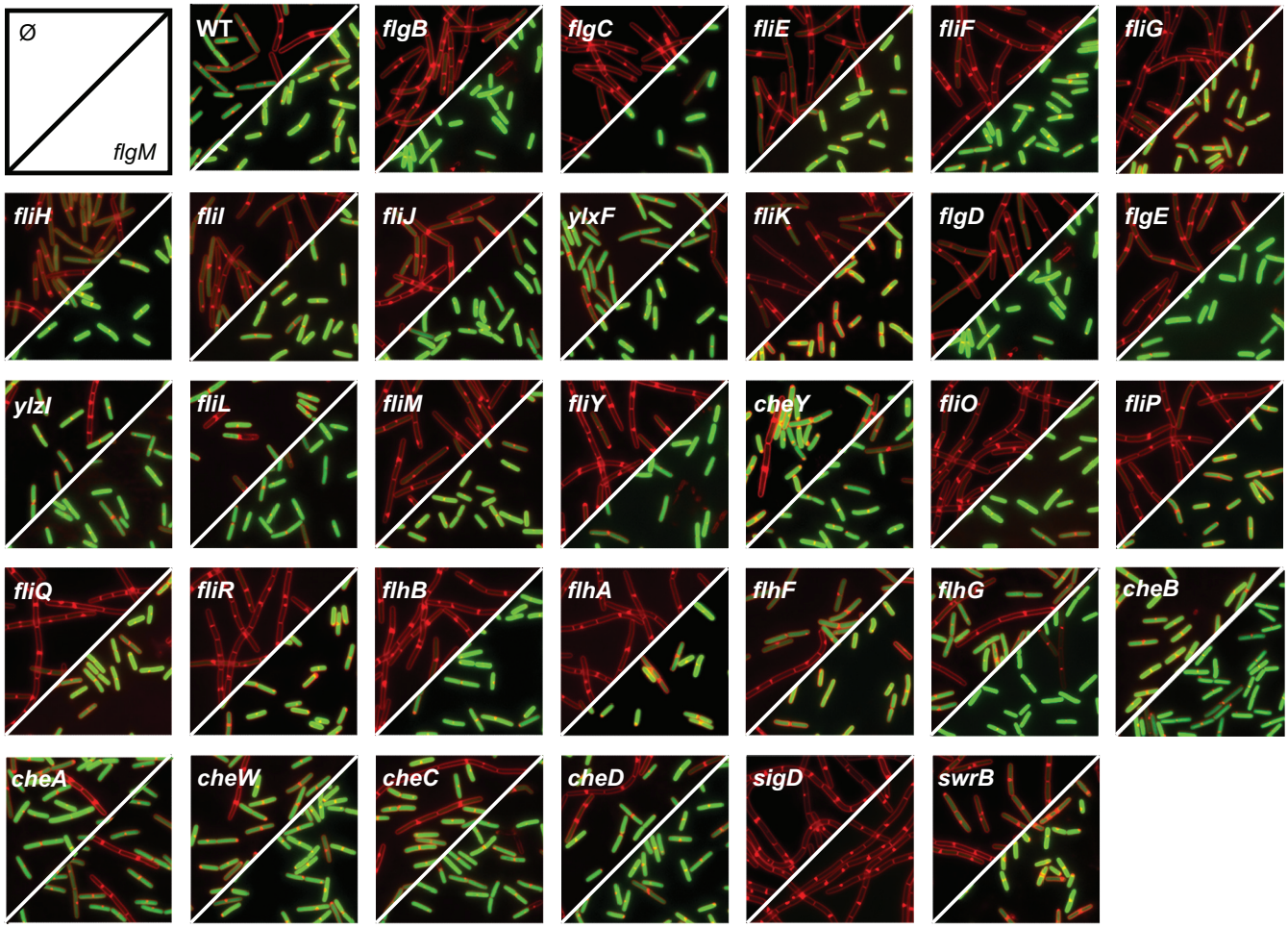

FIG 5 Mutations in the *fla-che* operon impair σ^D-dependent gene expression. Fluorescence microscopy of the indicated strains that contain the *amyE*::P_{hag}-GFP reporter construct. The top left triangle of each square is an image of the strain containing an in-frame deletion of the indicated gene; the bottom right triangle is an image of the corresponding deletion mutant strain containing an additional *flgM*::*tet* mutation (see the legend in the top left panel). Cell membranes were stained with FM4-64 and are false-colored red. GFP fluorescence is false-colored green. Scale bar, 4 μm. The following strains (mutated genes in parentheses) were used to generate the figure: DS908 (WT strain), DS4264 (*flgM*), DS7684 (*flgB*), DK1856 (*flgB flgM*), DS7685 (*flgC*), DK1857 (*flgC flgM*), DS7686 (*fliE*), DK1858 (*fliE flgM*), DS7687 (*fliF*), DS7457 (*fliF flgM*), DS7688 (*fliG*), DK1859 (*fliG flgM*), DS7689 (*fliH*), DK1860 (*fliH flgM*), DS7690 (*fliI*), DK1861 (*fliI flgM*), DS7691 (*fliJ*), DK1862 (*fliJ flgM*), DS7692 (*ylxF*), DK1863 (*ylxF flgM*), DS7693 (*fliK*), DK1864 (*fliK flgM*), DS7694 (*flgD*), DK1865 (*flgD flgM*), DS7695 (*flgE*), DK1866 (*flgE flgM*), DS7696 (*ylzI*), DK1867 (*ylzI flgM*), DS7697 (*fliL*), DK1868 (*fliL flgM*), DS7698 (*fliM*), DK1869 (*fliM flgM*), DS7699 (*fliY*), DK1870 (*fliY flgM*), DS7700 (*cheY*), DK1871 (*cheY flgM*), DS7701 (*fliO*), DK1872 (*fliO flgM*), DS7702 (*fliP*), DK1873 (*fliP flgM*), DS7703 (*fliQ*), DK1874 (*fliQ flgM*), DS7704 (*fliR*), DK1875 (*fliR flgM*), DS7705 (*flhB*), DK1876 (*flhB flgM*), DS7706 (*flhA*), DK1877 (*flhA flgM*), DS7707 (*flhF*), DK1878 (*flhF flgM*), DS7708 (*flhG*), DK1879 (*flhG flgM*), DS7709 (*cheB*), DK1880 (*cheB flgM*), DS7710 (*cheA*), DK1881 (*cheA flgM*), DS7711 (*cheW*), DK1882 (*cheW flgM*), DS7712 (*cheC*), DK1883 (*cheC flgM*), DS7713 (*cheD*), DK1884 (*cheD flgM*), DS7714 (*sigD*), DK1885 (*sigD flgM*), DS7715 (*swrB*), and DK1886 (*swrB flgM*).

portantly, FlgM secretion was reduced in each mutant background that also exhibited low σ^D-dependent gene expression (Fig. 1E). We conclude that the ability to activate σ^D is correlated with the ability to secrete FlgM into the extracellular environment.

In *B. subtilis*, the expression of FlgM is under explicit control of σ^D, and thus the reduced ability of some mutants to inhibit FlgM could limit FlgM expression and thus lower FlgM levels, both intracellularly and extracellularly, below the limit of detection (18, 47). To override native transcriptional regulation of FlgM, the *flgM* gene was artificially expressed from the artificial, IPTG-inducible P_{hyspank} promoter ($P_{hyspank}$-*flgM*) in each of the *fla-che* operon mutants in the Δ7 protease mutant background. FlgM secretion was abolished in cells mutated for the FliF and FliG basal body components, the FliO, FliP, FliQ, FliR, FlhA, and FlhB type III export apparatus components, and the FliK substrate specificity switch regulator (Fig 6B). By contrast, the remaining proteins required for hook-basal body completion were not essential for FlgM secretion when FlgM was artificially expressed (Fig 6B). We conclude that completion of the hook-basal body structural assembly intermediate enhances but is not absolutely required for FlgM secretion (Fig. 1E).

DISCUSSION

Flagellar biosynthesis is complex, and FlgM secretion is a paradigm for the morphogenetic coupling of flagellar structure and gene transcription (4). Prior to completion of the hook-basal body structural intermediate, FlgM inhibits the expression of the σ^D regulon such that the gene encoding the abundant flagellar filament protein Hag is not expressed prematurely (18, 30–33). In *S. enterica*, the flagellar type III export apparatus changes substrate

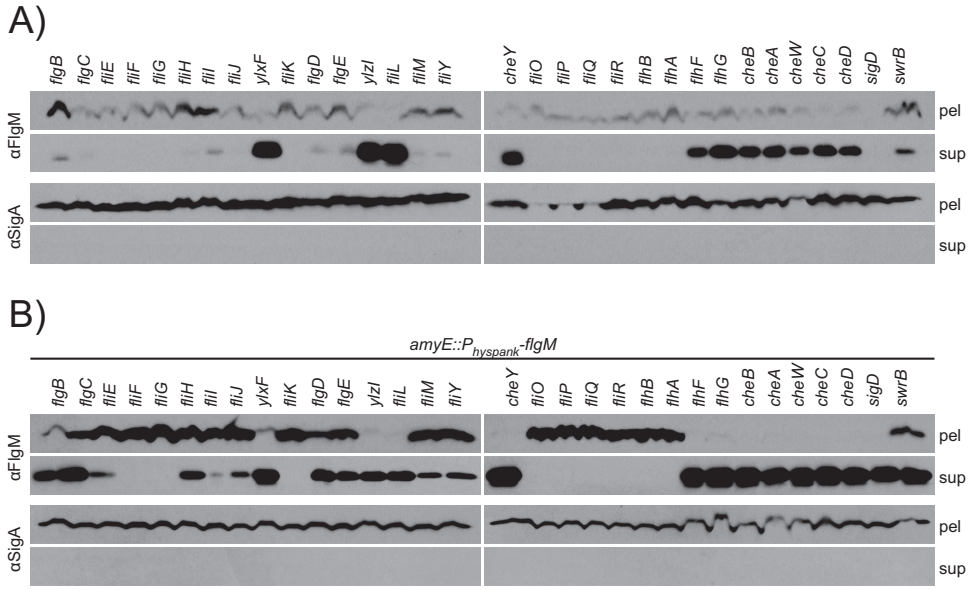

FIG 6 Mutations in the *fla-che* operon abolish FlgM secretion. (A) FlgM secretion assay in which control of FlgM is under the native promoter. All mutations were constructed in the Δ7 protease mutant background. The two panels were generated using the same samples. Blots were probed with both anti-FlgM (αFlgM) and anti-SigA (αSigA) to serve as a loading and lysis control. The strains with mutations for *flgB* (DK717), *flgC* (DS8404), *fliE* (DK2012), *fliF* (DS6871), *fliG* (DK1902), *fliH* (DK1951), *fliI* (DK2058), *fliJ* (DK1952), *ylxF* (DK2026), *fliK* (DK1971), *flgD* (DK1970), *flgE* (DS8365), *ylzI* (DK2014), *fliL* (DK2028), *fliM* (DK1953), *fliY* (DK1904), *cheY* (DK2031), *fliO* (DK1969), *fliP* (DK2059), *fliQ* (DK1903), *fliR* (DK3076), *flhB* (DK1968), *flhA* (DS8117), *flhF* (DK3077), *flhG* (DK2071), *cheB* (DK2060), *cheA* (DK2013), *cheW* (DK2030), *cheC* (DK2027), *cheD* (DK2029), *sigD* (DK2230), and *swrB* (DK3075) were used to generate the figure. (B) FlgM secretion assay in which FlgM is artificially expressed from an IPTG-inducible promoter. Strains contain the *amyE*::$P_{hyspank}$-*flgM* construct (*flgM*$^{++}$) and were grown in the presence of 1 mM IPTG. The strains with mutations *flgB flgM*$^{++}$ (DK3051), *flgC flgM*$^{++}$ (DK1143), *fliE flgM*$^{++}$ (DK3053), *fliF flgM*$^{++}$ (DS6919), *fliG flgM*$^{++}$ (DK3054), *fliH flgM*$^{++}$ (DK3052), *fliI flgM*$^{++}$ (DK3055), *fliJ flgM*$^{++}$ (DK3056), *ylxF flgM*$^{++}$ (DK3057), *fliK flgM*$^{++}$ (DK3058), *flgD flgM*$^{++}$ (DK3059), *flgE flgM*$^{++}$ (DK1144), *ylzI flgM*$^{++}$ (DK3060), *fliL flgM*$^{++}$ (DK3061), *fliM flgM*$^{++}$ (DK3062), *fliY flgM*$^{++}$ (DK3063), *cheY flgM*$^{++}$ (DK3064), *fliO flgM*$^{++}$ (DK3065), *fliP flgM*$^{++}$ (DK3066), *fliQ flgM*$^{++}$ (DK3067), *fliR flgM*$^{++}$ (DK3079), *flhB flgM*$^{++}$ (DK3068), *flhA flgM*$^{++}$ (DK1142), *flhF flgM*$^{++}$ (DK3080), *flhG flgM*$^{++}$ (DK3069), *cheB flgM*$^{++}$ (DK3070), *cheA flgM*$^{++}$ (DK3071), *cheW flgM*$^{++}$ (DK3072), *cheC flgM*$^{++}$ (DK3073), *cheD flgM*$^{++}$ (DK3074), *sigD flgM*$^{++}$ (DK2301), and *swrB flgM*$^{++}$ (DK3078) were used to generate the figure.

specificity upon hook-basal body completion to recognize, export, and inhibit FlgM (13, 14). While the FlgM paradigm is widely accepted, it has rarely been tested outside a subset of Gram-negative gammaproteobacteria (16). Here we show that the Gram-positive bacterium *B. subtilis* conforms to the established paradigm of flagellar morphogenetic coupling, as the activity of σ^D was tightly correlated with the ability to efficiently secrete FlgM from the cytoplasm.

FlgM secretion was not originally detected in the wild type due to the fact that FlgM was degraded by Epr and WprA, two relatively understudied representatives of the seven extracellular proteases secreted by *B. subtilis*. The mechanisms that govern extracellular protease specificity are unclear, so why FlgM is degraded by those two enzymes in particular and not by the general specificity protease AprE (subtilisin) is unknown (39). While the involvement of Epr and WprA may be arbitrary, it is also possible that protease-specific degradation of FlgM is biologically relevant. For example, Epr is the only protease expressed under the control of σ^D (48), and WprA (wall protease A) is anchored to the peptidoglycan and thus is in close proximity to the flagellar basal body (44). We note that the same two proteases, Epr and WprA, were reported to proteolytically restrict localization of the autolysin LytF, which is required for separating daughter cells after division, and LytF is coincidentally under strict σ^D control (46, 49). Proteolysis of FlgM and LytF suggests that at least some members of the σ^D regulon may be coordinately processed at the posttranslational level, but if so, the coprocessing seems unrelated to both motility and cell separation, as here we show that strains with deletion of all seven proteases produce single motile cells, comparable to what occurs in the wild type (see Fig. S1 in the supplemental material). The relevance of FlgM and/or LytF extracellular proteolysis is unknown.

It has been shown that mutation of a subset of *fla-che* operon genes abolishes σ^D-dependent gene expression in an FlgM-dependent manner (31–33). To further explore this correlation, we tested mutations of every gene in the *fla-che* operon and measured both motility and σ^D-dependent gene expression. Mutation of 24 of the 32 *fla-che* operon genes resulted in severe swarming motility defects. Four of the mutants defective for swarming motility expressed σ^D-dependent genes and were proficient for swimming in liquid (*swrB*, *cheA*, *cheY*, and *ylzI*), suggesting that the corresponding gene products were not essential for hook-basal body assembly. The remaining 20 genes were defective for both swarming and σ^D-dependent gene expression, and with the exceptions of *sigD* and *fliK*, all were predicted to encode a conserved structural component of the flagellum (20). Furthermore, each mutant defective for σ^D-dependent gene expression also failed to secrete FlgM. Thus, as in *S. enterica*, the ability to secrete FlgM depended on hook-basal body completion and FlgM secretion was tightly correlated with σ^D activity.

FlgM is autoinhibitory, as the *flgM* gene is expressed by σ^D (18). Thus, reduced FlgM secretion could be misinterpreted due

to reduced FlgM expression. Indeed, artificial IPTG induction of FlgM revealed that many genes required for hook-basal body assembly improved but were not in fact absolutely essential for FlgM secretion. Ultimately, nine gene products, including the flagellar baseplate FliF, the flagellar rotor FliG, the flagellar type III export apparatus components FliO, FliP, FliQ, FliR, FlhB, and FlhA, and the substrate specificity switch mediator FliK constituted the minimal set of proteins strictly required to secrete FlgM. In contrast, the completion of the hook-basal body, including the rod (FlgB and FlgC), the hook (FlgD and FlgE), the C-ring (FliM and FliY), and the C-rod (FliH, FliI, and FliJ), strongly enhances, but is not strictly essential, for FliK to switch the specificity of the type III export apparatus and permit FlgM secretion. We note that this may be the first report of robust FlgM secretion in the absence of a complete hook-basal body, perhaps due to the technical limitations of the Gram-negative model systems. In contrast, Gram-positive model organisms such as *B. subtilis* permit the study of early events in type III export as the substrates are secreted directly into the extracellular environment even in flagellar mutants with severe structural defects.

In sum, the control of FlgM in *B. subtilis* largely adheres to the paradigm of morphogenetic coupling of structural assembly and gene regulation established in *S. enterica*. In *S. enterica*, however, FlgM is believed to be the primary form of regulation on the expression of the flagellar filament protein; in *B. subtilis*, the flagellar filament protein Hag is regulated posttranscriptionally by CsrA, an RNA-binding protein that inhibits Hag translation (31, 50). Importantly, like FlgM, CsrA is controlled (albeit indirectly) by the activity of the flagellar type III export apparatus and completion of the hook-basal body (31, 50). Thus, *B. subtilis* engages both FlgM and CsrA during the assembly of the flagellum, but unlike CsrA, which is specific for one protein, FlgM controls an entire regulon of genes. Perhaps FlgM inhibition by secretion through the completed hook-basal body has less to do with regulating motility *per se* and more to do with coordinating motility gene expression with other aspects of *B. subtilis* biology, peptidoglycan hydrolases in particular.

ACKNOWLEDGMENTS

This work was supported by NIH Training Grant T32 GM007757 to R.A.C. and NIH GM093030 to D.B.K.

REFERENCES

1. **Wösten MMSM.** 1998. Eubacterial sigma-factors. FEMS Microbiol Rev **22:**127–150. http://dx.doi.org/10.1016/S0168-6445(98)00011-4.
2. **Haldenwang WG.** 1995. The sigma factors of *Bacillus subtilis*. Microbiol Rev **59:**1–30.
3. **Hughes KT, Mathee K.** 1998. The anti-sigma factors. Annu Rev Microbiol **52:**231–286. http://dx.doi.org/10.1146/annurev.micro.52.1.231.
4. **Chilcott GS, Hughes KT.** 2000. Coupling of flagellar gene expression to flagellar assembly in *Salmonella enterica* serovar Typhimurium and *Escherichia coli*. Microbiol Mol Biol Rev **64:**694–708. http://dx.doi.org/10.1128/MMBR.64.4.694-708.2000.
5. **Macnab RM.** 1992. Genetics and biogenesis of bacterial flagella. Annu Rev Genet **26:**131–158. http://dx.doi.org/10.1146/annurev.ge.26.120192.001023.
6. **Chevance FFV, Hughes KT.** 2008. Coordinating assembly of a bacterial macromolecular machine. Nat Rev Microbiol **6:**455–465. http://dx.doi.org/10.1038/nrmicro1887.
7. **Gillen KL, Hughes KT.** 1991. Negative regulatory loci coupling flagellin synthesis to flagellar assembly in *Salmonella typhimurium*. J Bacteriol **173:**2301–2310.
8. **Ohnishi K, Kutsukake K, Suzuki H, Iino T.** 1992. A novel transcriptional regulation mechanism in the flagellar regulon of *Salmonella typhimurium*: an anti-sigma factor inhibits the activity of the flagellum-specific sigma factor, σ^F. Mol Microbiol **6:**3149–3157. http://dx.doi.org/10.1111/j.1365-2958.1992.tb01771.x.
9. **Sorenson MK, Ray SS, Darst SA.** 2004. Crystal structure of the flagellar σ/anti-σ complex σ^{28}/FlgM reveals an intact σ factor in an inactive conformation. Mol Cell **14:**127–138. http://dx.doi.org/10.1016/S1097-2765(04)00150-9.
10. **Moriya N, Minamino T, Hughes KT, Macnab RM, Namba K.** 2006. The type III flagellar export specificity switch is dependent on FliK ruler and a molecular clock. J Mol Biol **359:**466–477. http://dx.doi.org/10.1016/j.jmb.2006.03.025.
11. **Minamino T, Moriya N, Hirano T, Hughes KT, Namba K.** 2009. Interaction of FliK with the bacterial flagellar hook is required for efficient export specificity switching. Mol Microbiol **74:**239–251. http://dx.doi.org/10.1111/j.1365-2958.2009.06871.x.
12. **Erhardt M, Singer HM, Wee DH, Keener JP, Hughes KT.** 2011. An infrequent molecular ruler controls flagellar hook length in *Salmonella enterica*. EMBO J **30:**2948–2961. http://dx.doi.org/10.1038/emboj.2011.185.
13. **Hughes KT, Gillen KL, Semon MJ, Karlinsey JE.** 1993. Sensing structural intermediates in bacterial flagellar assembly by export of a negative regulator. Science **262:**1277–1280. http://dx.doi.org/10.1126/science.8235660.
14. **Kutsukake K.** 1994. Excretion of the anti-sigma factor through a flagellar substructure couples flagellar gene expression with flagellar assembly in *Salmonella typhimurium*. Mol Gen Genet **243:**605–612.
15. **Karlinsey JE, Tanaka S, Bettenworth V, Yamaguchi S, Boos W, Aizawa S, Hughes KT.** 2000. Completion of the hook-basal body complex of the *Salmonella typhimurium* flagellum is coupled to FlgM secretion and *fliC* transcription. Mol Microbiol **37:**1220–1231. http://dx.doi.org/10.1046/j.1365-2958.2000.02081.x.
16. **Rust M, Borchert S, Niehus E, Kuehne SA, Gripp E, Bajceta A, McMurry JL, Suerbaum S, Hughes KT, Josenhans C.** 2009. The *Helicobacter pylori* anti-sigma factor FlgM is predominantly cytoplasmic and cooperates with the flagellar basal body protein FlhA. J Bacteriol **191:**4824–4834. http://dx.doi.org/10.1128/JB.00018-09.
17. **Helmann JD, Márquez LM, Chamberlin MJ.** 1988. Cloning, sequencing, and disruption of the *Bacillus subtilis* σ^{28} gene. J Bacteriol **170:**1568–1574.
18. **Mirel DB, Lauer P, Chamberlin MJ.** 1994. Identification of flagellar synthesis regulatory and structural genes in a σ^D-dependent operon of *Bacillus subtilis*. J Bacteriol **176:**4492–4500.
19. **Bertero MG, Gonzales B, Tarricone C, Ceciliani F, Galizzi A.** 1999. Overproduction and characterization of the *Bacillus subtilis* anti-sigma factor FlgM. J Biol Chem **274:**12103–12107. http://dx.doi.org/10.1074/jbc.274.17.12103.
20. **Albertini AM, Caramori T, Crabb WD, Scoffone F, Galizzi A.** 1991. The *flaA* locus of *Bacillus subtilis* is part of a large operon coding for flagellar structures, motility functions, and an ATPase-like polypeptide. J Bacteriol **173:**3573–3579.
21. **Márquez-Magaña LM, Chamberlin MJ.** 1994. Characterization of the *sigD* transcription unit of *Bacillus subtilis*. J Bacteriol **176:**2427–2434.
22. **Estacio W, Santa Anna-Arriola S, Adedipe M, Márquez-Magaña LM.** 1998. Dual promoters are responsible for transcription initiation of the *fla/che* operon in *Bacillus subtilis*. J Bacteriol **180:**3548–3555.
23. **West JT, Estacio W, Márquez-Magaña LM.** 2000. Relative roles of the *fla/che* P_A, P_{D-3}, and P_{sigD} promoters in regulating motility and *sigD* expression in *Bacillus subtilis*. J Bacteriol **182:**4841–4848. http://dx.doi.org/10.1128/JB.182.17.4841-4848.2000.
24. **Mirel DB, Chamberlin MJ.** 1989. The *Bacillus subtilis* flagellin gene (*hag*) is transcribed by the σ^{28} form of RNA polymerase. J Bacteriol **171:**3095–3101.
25. **Mirel DB, Lustre VM, Chamberlin MJ.** 1992. An operon of *Bacillus subtilis* motility genes transcribed by the σ^D form of RNA polymerase. J Bacteriol **174:**4197–4204.
26. **Kuroda A, Sekiguchi J.** 1993. High-level transcription of the major *Bacillus subtilis* autolysin operon depends on expression of the sigma D gene and is affected by a *sin* (*flaD*) mutation. J Bacteriol **175:**795–801.
27. **Serizawa M, Yamamoto H, Yamaguchi H, Fujita Y, Kobayashi K, Ogasawara N, Sekiguchi J.** 2004. Systematic analysis of SigD-regulated genes in *Bacillus subtilis* by DNA microarray and Northern blotting analyses. Gene **329:**125–136. http://dx.doi.org/10.1016/j.gene.2003.12.024.
28. **Kearns DB, Losick R.** 2005. Cell population heterogeneity during growth of *Bacillus subtilis*. Genes Dev **19:**3083–3094. http://dx.doi.org/10.1101/gad.1373905.
29. **Márquez LM, Helmann JD, Ferrari E, Parker HM, Ordal GW, Cham-**

berlin MJ. 1990. Studies of σ^D-dependent functions in *Bacillus subtilis*. J Bacteriol **172:**3435–3443.
30. **Caramori T, Barilla D, Nessi C, Sacchi L, Galizzi A.** 1996. Role of FlgM in σ^D-dependent gene expression in *Bacillus subtilis*. J Bacteriol **178:**3113–3118.
31. **Mukherjee S, Yakhnin H, Kysela D, Sokoloski J, Babitzke P, Kearns DB.** 2011. CsrA-FliW interaction governs flagellin homeostasis and a checkpoint on flagellar morphogenesis in *Bacillus subtilis*. Mol Microbiol **82:**447–461. http://dx.doi.org/10.1111/j.1365-2958.2011.07822.x.
32. **Courtney CR, Cozy LM, Kearns DB.** 2012. Molecular characterization of the flagellar hook in *Bacillus subtilis*. J Bacteriol **194:**4619–4629. http://dx.doi.org/10.1128/JB.00444-12.
33. **Cozy LM, Kearns DB.** 2010. Gene position in a long operon governs motility development in *Bacillus subtilis*. Mol Microbiol **76:**273–285. http://dx.doi.org/10.1111/j.1365-2958.2010.07112.x.
34. **Yasbin RE, Young FE.** 1974. Transduction in *Bacillus subtilis* by bacteriophage SPP1. J Virol **14:**1343–1348.
35. **Patrick JE, Kearns DB.** 2008. MinJ (YvjD) is a topological determinant of cell division in *Bacillus subtilis*. Mol Microbiol **70:**1166–1179. http://dx.doi.org/10.1111/j.1365-2958.2008.06469.x.
36. **Guérout-Fleury AM, Shazand K, Frandsen N, Stragier P.** 1995. Antibiotic-resistance cassettes for *Bacillus subtilis*. Gene **167:**335–336. http://dx.doi.org/10.1016/0378-1119(95)00652-4.
37. **Ben-Yehuda S, Rudner DZ, Losick R.** 2003. RacA, a bacterial protein that anchors chromosomes to the cell poles. Science **299:**532–536. http://dx.doi.org/10.1126/science.1079914.
38. **Bendezú FO, Hale CA, Bernhardt TG, de Boer PA.** 2009. RodZ (YfgA) is required for proper assembly of the MreB actin cytoskeleton and cell shape in *E. coli*. EMBO J **28:**193–204. http://dx.doi.org/10.1038/emboj.2008.264.
39. **Stahl ML, Ferrari E.** 1984. Replacement of the *Bacillus subtilis* subtilisin structural gene with an *in vitro*-derived deletion mutation. J Bacteriol **158:**411–418.
40. **Yang MY, Ferrari E, Henner DJ.** 1984. Cloning of the neutral protease gene of *Bacillus subtilis* and the use of the cloned gene to create an *in vitro*-derived deletion mutation. J Bacteriol **160:**15–21.
41. **Wu XC, Nathoo S, Pang AS, Carne T, Wong SL.** 1990. Cloning, genetic organization, and characterization of a structural gene encoding bacillopeptidase F from *Bacillus subtilis*. J Biol Chem **265:**6845–6850.
42. **Brückner R, Shoseyov O, Doi RH.** 1990. Multiple active forms of a novel serine protease from *Bacillus subtilis*. Mol Gen Genet **221:**486–490.
43. **Sloma A, Rufo GA, Theriault KA, Dwyer M, Wilson SW, Pero J.** 1991. Cloning and characterization of the gene for an additional extracellular serine protease of *Bacillus subtilis*. J Bacteriol **173:**6889–6895.
44. **Margot P, Karamata D.** 1996. The *wprA* gene of *Bacillus subtilis* 168, expressed during exponential growth, encodes a cell-wall associated protease. Microbiology **142:**3437–3444. http://dx.doi.org/10.1099/13500872-142-12-3437.
45. **Rufo GA, Sullivan BJ, Sloma A, Pero J.** 1990. Isolation and characterization of a novel extracellular metalloprotease from *Bacillus subtilis*. J Bacteriol **172:**1019–1023.
46. **Chen RC, Guttenplan SB, Blair KM, Kearns DB.** 2009. Role of the σ^D-dependent autolysins in *Bacillus subtilis* population heterogeneity. J Bacteriol **191:**5775–5784. http://dx.doi.org/10.1128/JB.00521-09.
47. **Hsueh Y-H, Cozy LM, Sham L-T, Calvo RA, Gutu AD, Winkler ME, Kearns DB.** 2011. DegU-phosphate activates expression of the anti-sigma factor FlgM in *Bacillus subtilis*. Mol Microbiol **81:**1092–1108. http://dx.doi.org/10.1111/j.1365-2958.2011.07755.x.
48. **Dixit M, Murudkar CS, Rao KK.** 2002. *epr* is transcribed from a σ^D promoter and is involved in swarming of *Bacillus subtilis*. J Bacteriol **184:**596–599. http://dx.doi.org/10.1128/JB.184.2.596-599.2002.
49. **Yamamoto H, Kurosawa S, Sekiguchi J.** 2003. Localization of the vegetative cell wall hydrolases LytC, LytE, and LytF on the *Bacillus subtilis* cell surface and the stability of these enzymes to cell wall-bound or extracellular proteases. J Bacteriol **185:**6666–6677. http://dx.doi.org/10.1128/JB.185.22.6666-6677.2003.
50. **Yakhnin H, Pandit P, Petty TJ, Baker CS, Romeo T, Babitzke P.** 2007. CsrA of *Bacillus subtilis* regulates translation initiation of the gene encoding the flagellin protein (*hag*) by blocking ribosome binding. Mol Microbiol **64:**1605–1620. http://dx.doi.org/10.1111/j.1365-2958.2007.05765.x.